NUREG/CR-6279

Application of Fracture Toughness Scaling Models to the Ductile-to-Brittle Transition

Prepared by
R. E. Link, J. A. Joyce

Naval Surface Warfare Center

U.S. Naval Academy

Prepared for
U.S. Nuclear Regulatory Commission

AVAILABILITY NOTICE

Availability of Reference Materials Cited in NRC Publications

Most documents cited in NRC publications will be available from one of the following sources:

1. The NRC Public Document Room, 2120 L Street, NW., Lower Level, Washington, DC 20555-0001

2. The Superintendent of Documents, U.S. Government Printing Office, P. O. Box 37082, Washington, DC 20402-9328

3. The National Technical Information Service, Springfield, VA 22161-0002

Although the listing that follows represents the majority of documents cited in NRC publications, it is not intended to be exhaustive.

Referenced documents available for inspection and copying for a fee from the NRC Public Document Room include NRC correspondence and internal NRC memoranda; NRC bulletins, circulars, information notices, inspection and investigation notices; licensee event reports; vendor reports and correspondence; Commission papers; and applicant and licensee documents and correspondence.

The following documents in the NUREG series are available for purchase from the Government Printing Office: formal NRC staff and contractor reports, NRC-sponsored conference proceedings, international agreement reports, grantee reports, and NRC booklets and brochures. Also available are regulatory guides, NRC regulations in the *Code of Federal Regulations*, and *Nuclear Regulatory Commission Issuances*.

Documents available from the National Technical Information Service include NUREG-series reports and technical reports prepared by other Federal agencies and reports prepared by the Atomic Energy Commission, forerunner agency to the Nuclear Regulatory Commission.

Documents available from public and special technical libraries include all open literature items, such as books, journal articles, and transactions. *Federal Register* notices, Federal and State legislation, and congressional reports can usually be obtained from these libraries.

Documents such as theses, dissertations, foreign reports and translations, and non-NRC conference proceedings are available for purchase from the organization sponsoring the publication cited.

Single copies of NRC draft reports are available free, to the extent of supply, upon written request to the Office of Administration, Distribution and Mail Services Section, U.S. Nuclear Regulatory Commission, Washington, DC 20555-0001.

Copies of industry codes and standards used in a substantive manner in the NRC regulatory process are maintained at the NRC Library, Two White Flint North, 11545 Rockville Pike, Rockville, MD 20852-2738, for use by the public. Codes and standards are usually copyrighted and may be purchased from the originating organization or, if they are American National Standards, from the American National Standards Institute, 1430 Broadway, New York, NY 10018-3308.

DISCLAIMER NOTICE

NUREG/CR-6279

Application of Fracture Toughness Scaling Models to the Ductile-to-Brittle Transition

Manuscript Completed: December 1995
Date Published: January 1996

Prepared by
R. E. Link, Naval Surface Warfare Center
J. A. Joyce, U.S. Naval Academy

Naval Surface Warfare Center
3-A Leggett Circle
Annapolis, MD 21402

U.S. Naval Academy
590 Holloway Road
Annapolis, MD 21402

S. N. Malik, NRC Project Manager

Prepared for
Division of Engineering Technology
Office of Nuclear Regulatory Research
U.S. Nuclear Regulatory Commission
Washington, DC 20555-0001
NRC Job Code J6036

ABSTRACT

An experimental investigation of fracture toughness in the ductile-brittle transition range was conducted. A large number of ASTM A533, Grade B steel, bend and tension specimens with varying crack lengths were tested throughout the transition region. Cleavage fracture toughness scaling models were utilized to correct the data for the loss of constraint in short crack specimens and tension geometries. The toughness scaling models were effective in reducing the scatter in the data, but tended to over-correct the results for the short crack bend specimens. A proposed ASTM Test Practice for Fracture Toughness in the Transition Range, which employs a master curve concept, was applied to the results. The proposed master curve over predicted the fracture toughness in the mid-transition and a modified master curve was developed that more accurately modeled the transition behavior of the material. Finally, the modified master curve and the fracture toughness scaling models were combined to predict the as-measured fracture toughness of the short crack bend and the tension specimens. It was shown that when the scaling models over correct the data for loss of constraint, they can also lead to non-conservative estimates of the increase in toughness for low constraint geometries.

TABLE OF CONTENTS

LIST OF FIGURES

LIST OF TABLES

ACKNOWLEDGEMENTS

The work described in this investigation was performed at the Annapolis Detachment of the Naval Surface Warfare Center and the U.S. Naval Academy as a part of the "Elastic-Plastic Fracture Mechanics Technology for LWR Alloys Program," sponsored by the U.S. Nuclear Regulatory Commission (USNRC). The support of the Materials Engineering Branch at the USNRC, especially the Program Technical Monitor, Dr. Shah Malik, is gratefully acknowledged. The authors would also like to acknowledge the technical contributions of Mr. Stanford Womack for performing many of the tests reported herein and Mr. Wayne Farmer for preparing many of the specimens tested in this investigation. Dr. R.H. Dodds, Jr. provided the numerical analysis and developed the cleavage fracture toughness scaling model for the SE(T) geometry that was reported herein.

OBJECTIVES

Fracture toughness scaling models and two parameter fracture mechanics methodologies have recently been developed to quantify and predict the effects of crack size, mode of loading, and specimen size on fracture toughness [1-4]. These new approaches have been used successfully to quantify the apparent increase in fracture toughness that is measured using specimens containing short cracks [1,5-7]. This paper describes an experimental investigation of the applicability of the fracture toughness scaling approach to an embrittled A533B steel, a material commonly used in commercial nuclear reactor pressure vessels. The test matrix consisted of 39 large (1.6T) bend specimens tested at temperatures corresponding to lower shelf, lower transition, mid-transition. One-half of the specimens contained short cracks, with a/W ratios of 0.1, while the remaining specimens were standard, deep-notched, a/W = 0.5 test specimens. In addition, some specimen halves were machined into standard 1T and shallow cracked 1T bend and tension specimens which were tested at the lower shelf, lower transition, and mid-transition temperatures. Since some of the specimens tested at the mid-transition temperature did not cleave, they represented upper shelf J-R curve results for this scale of test specimen and no higher temperature was needed. Eight repeat tests for each specimen geometry were conducted at the lower transition and mid-transition temperatures so that statistical methods could be used to evaluate a median transition temperature curve, and meaningful confidence limits could be evaluated. The statistical method used is that of the proposed test practice[1] developed recently by the ASTM Task Group E08.08.03. This method uses a Weibull probability distribution approach to develop a "Master Curve" from a data set at one lower transition temperature, and then is a representation of the ductile to brittle transition at all temperatures, at least up to the ductile, upper shelf K_{JIc}. Since this method has not yet been widely distributed it will be carefully described below.

1.0 EXPERIMENTAL DETAILS

1.1 Material Description

The material used in this investigation was ASTM A533, Grade B steel from a plate with dimensions of 6.9 m x 3.3 m x 0.18 m (273 in. x 128 in. x 7 in.). The chemical composition and as-received mechanical properties for the plate are presented in Table 1. The plate was subjected to a heat treatment which was intended to simulate the increase in strength and transition temperature due to irradiation. The heat treatment consisted of austenitizing at 900°C (1650°F) for 7.5 hrs, followed by a water quench and then tempered at 510°C (950°F) for 3 hours and air cooled. The resulting microstructure

[1]"Test Practice for Fracture Toughness in the Transition Range," Draft 5, dated March 3, 1993, ASTM Task Group E08.08.03.

Table 1 Chemical composition and as-received mechanical properties of the ASTM A533, Grade B steel plate used in this investigation.

Element	weight percent
Carbon	0.18
Manganese	1.27
Phosphorous	0.014
Sulfur	0.015
Silicon	0.24
Nickel	0.63
Molybdenum	0.54
Iron	Bal.
0.2% Yield Strength, MPa (ksi)	538 (78)
Ultimate Tensile Strength, Mpa (ksi)	607 (88)
Elongation in 51 mm, %	23
Nil Ductility Temperature, °C (°F)	-29 (-20)

was bainitic with an ASTM grain size of 5-6. It was understood that the mechanism for radiation embrittlement is not the same as that resulting from the heat treatment. Following heat treatment, the mechanical properties of the plate were determined at several positions through the thickness of the plate. These results are presented in Table 2. As a result of the heat treatment, the transition temperature, as indicated by the nil-ductility transition (NDT) temperature, was shifted 10°C higher and the tensile strength was increased about 20%. There is also a strength gradient through the thickness of the plate, with the material near the surface being slightly higher in strength than the material in the middle of the plate thickness.

Charpy V-notch impact toughness transition curves were determined for material removed from the surface and quarter-thickness locations in the heat treated plate. The transition curves are plotted in Figure 1. The Charpy curves do not give a clear indication of the difference in transition temperature between the surface and quarter-thickness material.

Table 2 Mechanical properties of ASTM A533, Gr. B steel plate after heat treatment.

	Near Surface	Quarter Thickness	Mid-thickness
0.2% Yield Strength, MPa (ksi)	607 (88)	579 (84)	579 (84)
Ultimate Tensile Strength, MPa (ksi)	745 (108)	724 (105)	731 (106)
% Elongation in 51 mm	23	23	22
Nil Ductility Temperature, °C (°F)	-7 (20)	4 (40)	Not determined

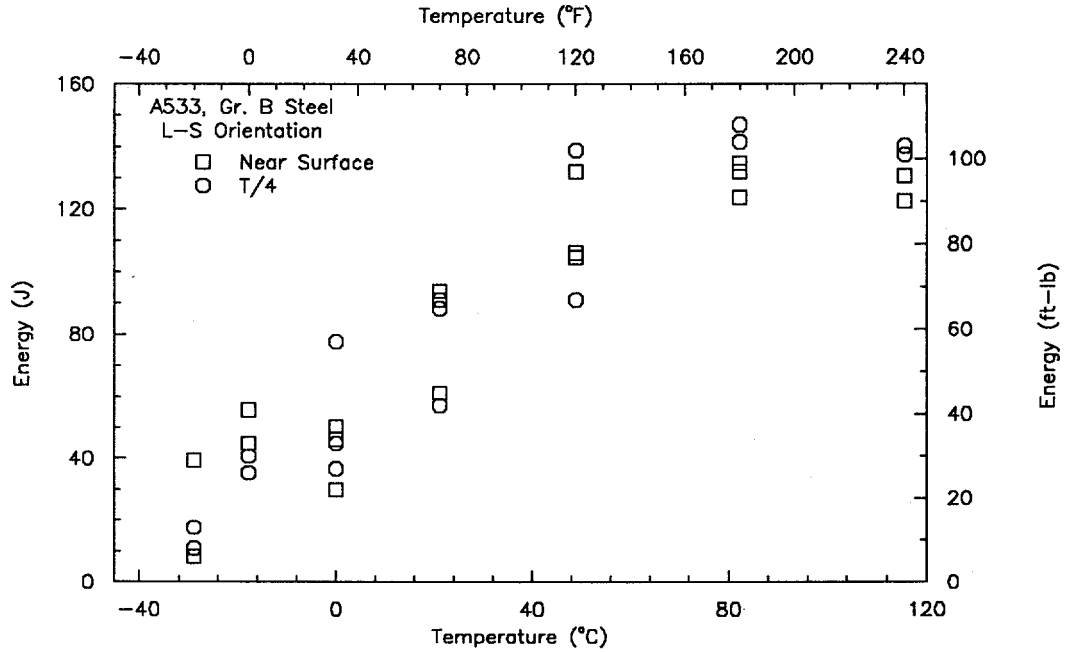

Figure 1 Charpy V-notch impact energy transition curves for specimens removed near the surface and from the quarter-thickness positions of the heat treated, ASTM A533, Gr. B steel plate.

1.2 Fracture Toughness Tests

One of the goals of this investigation was to measure the fracture toughness over the full ductile to brittle transition. It was desired to conduct tests at temperatures corresponding to the upper and lower shelf, lower transition where failure would occur by cleavage with little or no prior ductile tearing and mid transition where failure would occur by cleavage after some stable tearing, beyond the J_{Ic} point. The following temperatures were used for tests of single edge notch bend (SE(B)) specimens: lower shelf @ -62°C (-80°F); lower transition @ -7°C (+20°F); mid transition @ 21°C (70°F).

SE(B) specimens were removed from the plate in the L-S orientation. The SE(B) specimens were removed from the plate so that the initial crack tip for all specimens was located at the quarter-thickness position. This was done to ensure that all specimens sampled material that had the same strength and microstructural characteristics. A total of 39 large SE(B) specimens were prepared, 19 with an initial crack size, a/W=0.1 and 20 with an initial crack size, a/W=0.55. The specimens had a nearly square cross-section and had dimensions of B=89 mm (3.5 in.), W=83 mm (3.25 in.), S=332 mm (13 in.) which corresponds to a 1.6T plan size. The crack starter notch was produced using wire electric discharge machining and had a width of 0.64 mm (0.025 in.). Prior to fatigue precracking, a single cycle of reversed bending was applied to the specimen to produce a compressive plastic zone and a residual tensile stress at the notch tip. The load level was selected to produce a plastic zone of 0.6 mm (0.025 in.). The specimens were precracked using the specimen compliance to estimate the crack length until the desired initial crack size was reached. The crack length was monitored using a computer controlled servo-hydraulic test machine, and the short crack compliance equation obtained by Joyce [8], until the final precrack length of approximately 8.3 mm (0.325 in.) was obtained. The total amount of fatigue crack extension from the machined notch was typically 1.9 mm (0.075 in.), approximately three times the size of the compressive plastic zone that was formed at the notch tip. This procedure yielded excellent results for the shallow cracked specimens that had an initial crack size of a/W=0.1. The crack fronts were uniform and straight as shown in Figure 2. Side grooves were machined into the specimen following precracking. The side groove depth was 5% of the specimen thickness on each side for a total thickness reduction of 10%.

1T SE(B) specimens were machined from the broken halves of the large SE(B) specimens. These specimens were also removed so that the crack tip was at the quarter thickness position. A similar precracking procedure was employed for the short crack 1T SE(B) specimens. For all SE(B) specimens, the testing procedure was in accordance with the requirements of the draft Standard Method for Fracture Toughness Testing[2], where applicable.

Single edge notched tensile specimens (SE(T)) were machined with the crack in the L-S orientation and the crack tip located at the plate quarter point. Specimen

---

[2] Standard Method for the Measurement of Fracture Toughness," Draft Standard, Version 13, American Society for Testing and Materials, Philadelphia, April 1993.

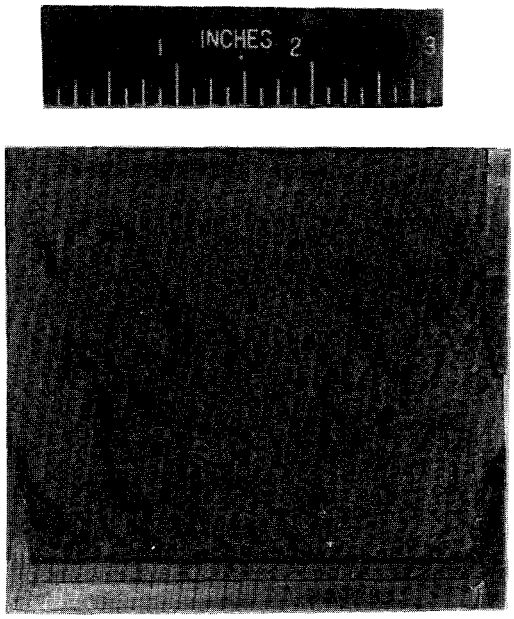

Figure 2 Photograph of fracture surface from 1.6T SE(B) specimen showing straight crack front and side groove depth.

dimensions were 63.5 by 305 mm., by 25.4 mm thick. The test section was 229 mm. in length, and the specimens were pin loaded with 25.4 mm diameter pins located on the specimen centerline. These specimens were precracked in bending to a crack depth of a/W=0.4 using a 193 mm (8 inch) bend span using the procedure of ASTM E1152. The specimens were tested using an unloading compliance method as described by Joyce, et al. [9]. For all tests, temperatures were maintained using a chamber which was capable of maintaining the temperature within 2 °C.

1.3 Test Technique

All tests were conducted using a single specimen, computer interactive, unloading compliance test procedure which allowed monitoring the specimen crack length and the applied J integral during the course of the test. Equations were presented in Joyce, et al. [9] for the required elastic and plastic components of the J integral and for estimating the crack length from the experimentally measured crack opening compliance and are presented in the next section. For the short crack SE(B) and the SE(T) specimens, crack growth corrected J equations are used here, as developed in Joyce, et al. [9], which are similar to those required by ASTM E1152 for the deep SE(B) specimens and the C(T) specimens. All data was stored on magnetic media for subsequent re-analysis as needed.

The SE(B) specimens were tested with standard three-point bend fixtures which were made much sturdier than usual to accommodate the higher loads typical of short

crack specimens. The procedures used for the short crack tests were presented by Joyce [8] which showed clearly that unloading compliance was a viable test technique for SE(B) specimens with a/W as short as 0.1. The compliance equations are much less sensitive in the short crack region, but the load applied increases with $(W-a)^2$ so that for the short crack specimens the unloadings become much larger, and the crack opening displacement (COD) continues to be adequately large and can be measured with a high resolution digital voltmeter. The combination of high loads and less sensitive unloading compliance makes these tests more difficult, but if care is taken, excellent results can be obtained. A flex bar was used to measure the load line displacements for all SE(B) specimens as described previously [10] since significant indentations did occur at the rollers for these specimens.

The SE(T) specimens were tested in a 1 MN hydraulic test machine with load line and COD gages to obtain the data needed for J and a/W estimation for this geometry. For the a/W = 0.4 crack length used, the constraint conditions in this specimen are intermediate to those of the short and deep notched SE(B) specimens.

2.0 ANALYSIS

2.1 J Integral Analysis

The J integral is calculated here by summing the elastic and plastic components, with the components calculated separately. The elastic J component, J_{el}, is calculated from:

$$J_{el} = \frac{K^2}{E'} \tag{1}$$

where K is the elastic stress intensity factor for the specimen, $E'=E/(1-\nu^2)$, and E and ν are the elastic modulus and Poisson's ratio, respectively. The plastic J component, J_{pl}, is calculated using the ASTM Standard E1152 J_{pl} equation:

$$J_{pl(i)} = J_{pl(i-1)} + \frac{\eta_i}{b_i}\left[\frac{A_{pl(i)} - A_{pl(i-1)}}{B_N}\right]\left[1 - \frac{\gamma_i\,(a_i - a_{(i-1)})}{b_i}\right] \tag{2}$$

with:

$A_{pl(i)}$= area under the load versus plastic load line displacement curve to increment i,
B_N = net specimen thickness at the side groove roots,
η_i = the plastic η factor at crack length a_i
b_i = the incremental remaining ligament
W = the specimen width and

$$\gamma_i = \left[\eta_i - 1 - \frac{b_i}{W}\frac{\eta_i'}{\eta_i}\right] \tag{3}$$

evaluated at the crack length a_i, and:

$$\eta_i' = d\eta_i/d(a_i/W) \tag{4}$$

2.2 SE(B) Analysis

Previous work by Joyce [8] has shown that unloading compliance can be used to evaluate J-R curves for short crack bend specimens. For the short crack specimens the crack length was estimated from:

$$\frac{a}{W} = 1.01878 - 4.5367u + 9.0101u^2 - 27.333u^3 + 74.4u^4 - 71.489u^5$$

$$u = \frac{1}{\left(\frac{B_e W E' C}{S/4}\right)^{1/2} + 1} \tag{5}$$

where: S = specimen bend span
$E' = E/(1 - \nu^2)$
C = crack mouth opening compliance

and:

$$B_e = B - \frac{(B - B_N)^2}{B} \tag{6}$$

which is accurate over the range $0.05 \leq a/W \leq 0.45$ within 1%. The standard equation of ASTM E1152 was used for the deep cracked bend specimens analyzed below.

For the deep cracked SE(B) specimens the η and γ factors of ASTM E1152, ($\eta = 2.0$ and $\gamma = 1.0$), are used in Eq. 2 to evaluate J. For the short crack specimens, however, these coefficients must be changed to accurately evaluate J. This problem has been investigated by Haigh and Richards [11], Sumpter [12], and by Joyce [8]. In the work that follows the polynomial function for η_i developed by Sumpter [12] is used for all short cracked SE(B) specimens with $a/W < 0.282$. This polynomial expression is:

$$\eta = 0.32 + 12(a/W) - 49.5(a/W)^2 + 99.8(a/W)^3 \quad (7)$$

This equation gives $\eta < 2.0$ for a/W < 0.282. When the crack length exceeds a/W = 0.282, the standard deep crack value, $\eta = 2.0$, is used. In this work the short crack specimens were started and completed with a/W < 0.282.

The γ factor is calculated from η using Eq. 3. For the short crack specimens γ was obtained by differentiating Eq. (7) to give:

$$\gamma = \frac{-12.22 + 106.7\left(\frac{a}{W}\right) - 236.6\left(\frac{a}{W}\right)^2 - 924.6\left(\frac{a}{W}\right)^3 + 4845.4\left(\frac{a}{W}\right)^4 - 9880\left(\frac{a}{W}\right)^5 + 9960\left(\frac{a}{W}\right)^6}{0.32 + 12\left(\frac{a}{W}\right) - 49.5\left(\frac{a}{W}\right)^2 + 99.8\left(\frac{a}{W}\right)^3} \quad (8)$$

2.3 SE(T) Analysis

Previous work by Joyce, et al. [9] has demonstrated that unloading compliance can be used to obtain J-R curves for single edge notched, SE(T), tensile specimens. For these specimens the crack length was estimated from:

$$\frac{a}{W} = 1.012525 - 2.95323u + 6.68u^2 - 17.1954u^3 + 25.3571u^4 - 12.9747u^5$$

$$u = \frac{1}{\left(B_e E' C\right)^{1/2} + 1} \quad (9)$$

For J integral evaluation the form of Eqs. 1 and 2 can be used with:

$$K = \sqrt{\pi a}\,\frac{P}{BW}\,F(a/W) \quad (10)$$

with

$$F(a/W) = -0.0917 + 22.392(a/W) - 141.96(a/W)^2 + 449.72(a/W)^3 - 645.59(a/W)^4 + 363.52(a/W)^5 \quad (11)$$

and the following expressions for η and γ taken from [9]

$$\eta_i = 5.71(a_i/W) \qquad 0 < a_i \leq 0.417 \qquad (12)$$

$$\eta_i = 2.38 \qquad 0.417 < a_i \leq 1.0 \qquad (13)$$

$$\gamma_i = \eta_i - 1 - (b_i/W)\left(\frac{5.71}{\eta_i}\right) \qquad 0 < a_i/W \leq 0.417 \qquad (14)$$

$$\gamma_i = 1.38 \qquad 0.417 < a_i/W \leq 1.0 \qquad (15)$$

3.0 Cleavage Fracture Toughness Scaling Models

Cleavage fracture toughness scaling models have been developed recently to account for variations in fracture toughness resulting from the loss of in-plane constraint due to specimen size and crack length [2]. The scaling model is a micromechanics-based approach that uses the concept of a critical stressed volume as a failure criterion. The stress distribution in a finite body is compared with that of an infinite body under small-scale yielding. As plasticity develops in the finite specimen geometry, the stresses at the crack tip are not as severe as those in the infinite body due to loss of constraint. Consequently, the specimen must be loaded to a higher J level to stress the same volume of material ahead of the crack tip to a particular critical level. Due to the self-similar nature of the crack-tip stress fields in the finite body, the ratio of J in the finite body, J_{FB}, to J under small scale yielding, J_{SSY}, is insensitive to the particular value selected for the critical stress [1]. The cleavage fracture toughness scaling models have been demonstrated on cleavage fracture toughness transition data for several structural steels [6,7] with excellent results. The increase in fracture toughness resulting from shallow cracks was well predicted, and the scatter in the data was reduced considerably by the application of the scaling model. It has been suggested that constraint corrections be applied to fracture toughness data before applying statistical analysis methods to the data [2] so that the statistics only account for the variation in fracture toughness which is due to material variability and not the effects of constraint.

3.1 Toughness Scaling Relationships

The stress distributions for the SSY case and the finite body case and the scaling models were determined using detailed 2-D, plane strain finite element analysis by Dodds, et al. [2][3]. The toughness scaling relationships are plotted in Figure 3 for two crack sizes in an SE(B) specimen and for an SE(T) specimen with a/W=0.4 for a material with n=10. The scaling relationships were digitized and curve-fit for convenience in calculating the constraint-corrected fracture toughness, J_{SSY}, for each specimen. The average difference between the digitized data and the curve fits was less than 2% over the range of deformation levels given with each equation below. In the following equations, b is the

[3] Results for the SE(T) specimen with a/W=0.4 were provided by R.H. Dodds, Jr. via private communication.

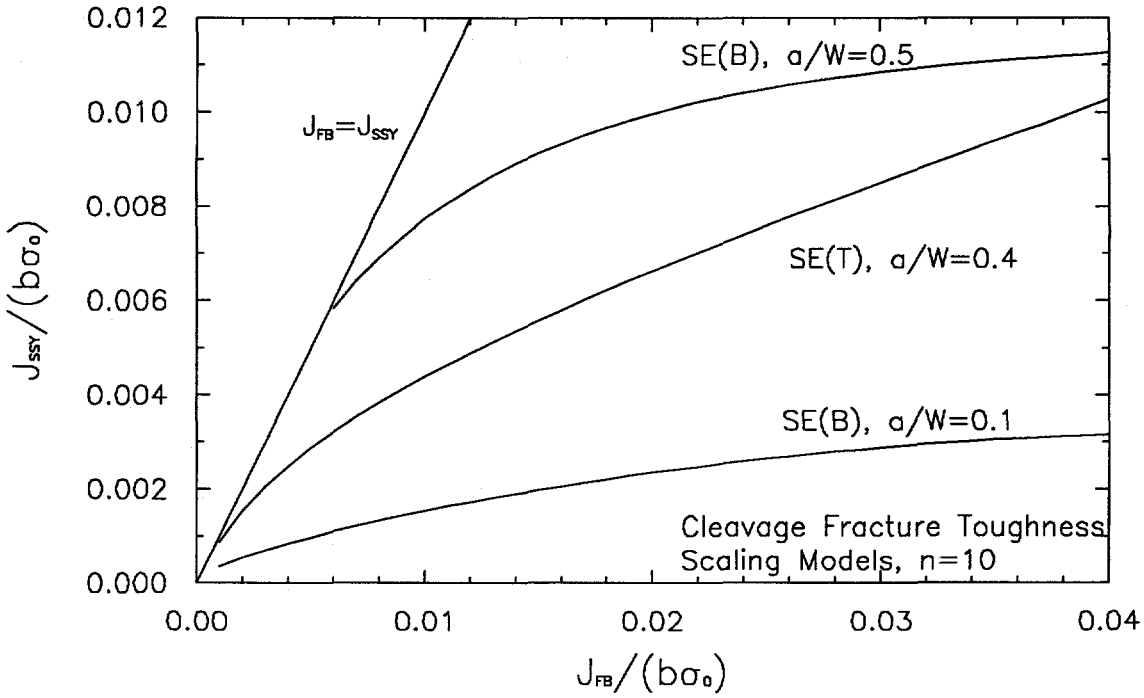

Figure 3 Cleavage fracture toughness scaling relationships for SE(B) specimens with a/W=0.1 and 0.5 and an SE(T) specimen with a/W=0.4 for a material with strain hardening coefficient, n=10.

remaining ligament and σ_o is the yield stress. For the SE(B) specimen with a/W=0.1,

$$\frac{J_{SSY}}{b\sigma_o} = 0.00919\left(\frac{J_{FB}}{b\sigma_o}\right)^{1/2} + 0.0722\left(\frac{J_{FB}}{b\sigma_o}\right) - 0.979\left(\frac{J_{FB}}{b\sigma_o}\right)^2 \quad (16)$$

for $J_{FB}/(b\sigma_o)<0.04$. For the SE(B) specimen with a/W=0.5

$$\frac{J_{SSY}}{b\sigma_o} = -0.0451\left(\frac{J_{FB}}{b\sigma_o}\right)^{0.25} + 0.3022\left(\frac{J_{FB}}{b\sigma_o}\right)^{0.5} - 0.8551\left(\frac{J_{FB}}{b\sigma_o}\right) + 3.246\left(\frac{J_{FB}}{b\sigma_o}\right)^2 \quad (17)$$

which is valid for $0.005 \le J_{FB}/(b\sigma_o) \le 0.04$. For $J_{FB}/(b\sigma_o) < 0.005$, $J_{SSY} = J_{FB}$

The cleavage fracture toughness scaling relationship for the SE(T) specimen with a/W=0.4 is given by:

$$\frac{J_{SSY}}{b\sigma_o} = -0.0079\left(\frac{J_{FB}}{b\sigma_o}\right)^{0.25} + 0.0748\left(\frac{J_{FB}}{b\sigma_o}\right)^{0.5} - 0.0692\left(\frac{J_{FB}}{b\sigma_o}\right) + 1.009\left(\frac{J_{FB}}{b\sigma_o}\right)^2 \quad (18)$$

for $J_{FB}/(b\sigma_o) < 0.04$.

The results for all of the tests conducted are summarized in Table 3 through Table 6, including the constraint-corrected toughness values and the equivalent K_J values. The results for all of the tests are plotted in Figure 4. In this program, all but two of the deeply-notched 1.6T SE(B) specimens tested below 21°C maintained SSY conditions until cleavage interruption occurred and required no correction. The remaining 1.6T SE(B) specimens and most of the 1T SE(B) and SE(T) specimens developed a considerable falloff in crack tip constraint before cleavage initiation occurred and had to be corrected. The corrected fracture toughness values from all of the tests which exhibited cleavage fracture are plotted in Figure 5. Comparison with Figure 4 shows that the SSY-corrected data exhibit considerably less scatter that the uncorrected data, apparently removing the effects of crack tip plasticity, geometry and loading mode from the fracture toughness values.

3.2 Transition Range Analysis Procedure

A recent proposed test practice of ASTM Subcommittee E08.08.03 is used here to analyze the results in the ductile to brittle transition range. The test practice starts with at least six replicated tests with a/W=0.5 at a single temperature in the lower or mid transition which are used to characterize the Weibull distribution for the data population. Stress intensity values, K_{Jc}, are used to measure the cleavage initiation toughness where J is obtained according to ASTM E1152, or from the short crack equations presented

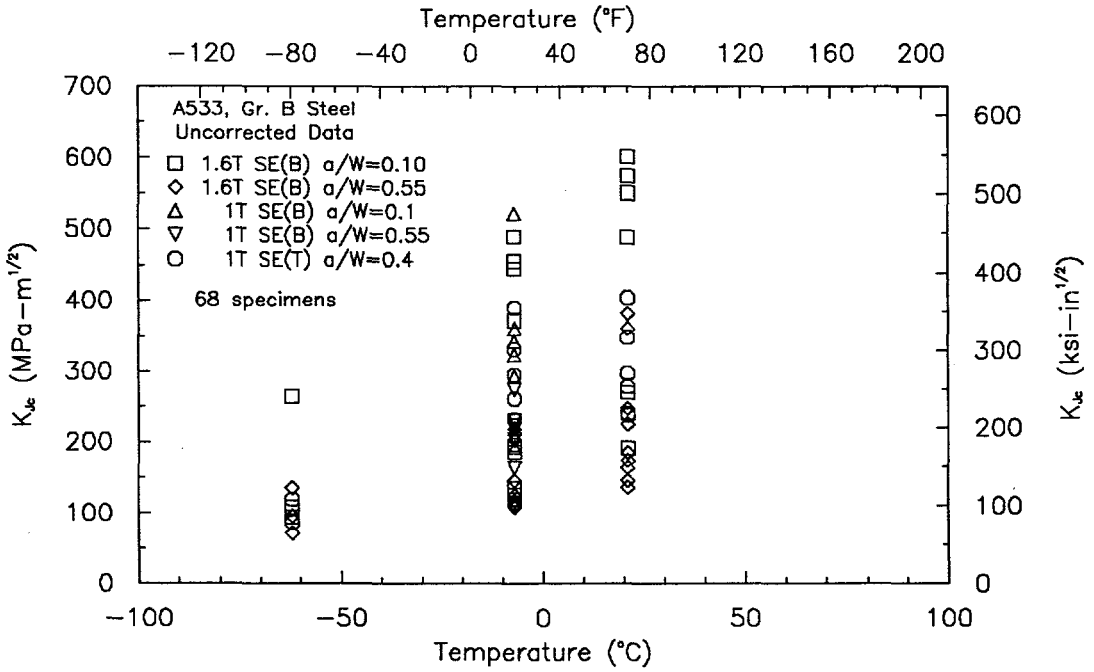

Figure 4 Fracture toughness as a function of temperature for all tests conducted in this investigation.

Table 3 Summary of results for 1.6T SE(B) specimens with a/W=0.55.

ID	Temp. (C)	a/W	W (mm)	a_o (mm)	Δa (mm)	J_{crit} (kJ/m^2)	J_{SSY} (kJ/m^2)	K_{Jcrit} (MPa-m$^{1/2}$)	K_{Jssy} (MPa-m$^{1/2}$)
B12	-62	0.55	83	45.1	0.0	25	25	71	71
B3	-62	0.55	83	45.5	0.0	93	93	136	136
B5	-62	0.56	83	45.9	0.0	47	47	97	97
B1	-7	0.54	83	44.7	0.0	59	59	109	109
B11	-7	0.55	83	45.5	0.0	79	79	126	126
B2	-7	0.55	83	45.1	0.0	209	165	204	182
B20	-7	0.56	83	46.3	0.0	107	107	146	146
B22	-7	0.55	83	45.6	0.0	63	63	112	112
B4	-7	0.55	83	45.6	0.0	241	176	220	188
B6	-7	0.55	83	45.7	0.0	70	70	118	118
B8	-7	0.56	83	46.2	0.0	64	64	113	113
B10	21	0.61	75	46.2	0.0	107	101	146	142
B14	21	0.55	83	45.7	3.1	661	233	363	216
B16	21	0.55	83	45.6	4.1	740	236	385	218
B17	21	0.55	83	45.5	0.0	175	149	187	173
B18	21	0.56	83	45.9	0.0	155	139	176	166
B21	21	0.55	83	45.8	0.0	93	93	137	137
B23	21	0.56	83	45.9	0.0	311	193	249	196
B15	21	0.56	83	45.9	0.0	137	128	165	160
B9	21	0.56	83	45.9	0.3	258	180	227	190

Table 4 Summary of results for 1.6T SE(B) specimens with a/W=0.1.

ID	Temp. (C)	a/W	W (mm)	a_o (mm)	Δa (mm)	J_{crit} (kJ/m^2)	J_{SSY} (kJ/m^2)	K_{Jcrit} (MPa-m$^{1/2}$)	K_{Jssy} (MPa-m$^{1/2}$)
C4	-62	0.10	83	8.4	0.0	59	19	108	62
C10	-62	0.10	83	8.4	0.0	45	16	95	57
C17	-62	0.10	83	8.4	0.0	354	58	266	109
C2	-7	0.10	83	8.4	0.0	92	25	135	70
C9	-7	0.10	83	8.3	0.0	79	23	126	67
C21	-7	0.11	83	8.7	0.0	175	37	187	86
C11	-7	0.10	83	8.3	0.9	701	90	374	134
C13	-7	0.10	83	8.4	1.6	1056	113	460	150
C19	-7	0.10	83	8.2	2.3	1219	121	494	155
C18	-7	0.11	83	8.7	1.9	1006	110	449	148
C8	-7	0.10	83	8.2	0.0	72	21	120	665
C14	21	0.10	83	8.3	4.1	1836	137	606	166
C6	21	0.11	83	8.7	8.8	...	...	...	...
C5	21	0.11	83	8.9	0.2	184	38	192	88
C20	21	0.10	83	8.3	2.9	1541	132	555	162
C7	21	0.11	83	8.7	5.6	1678	134	579	164
C15	21	0.10	83	8.5	2.4	1211	120	492	155
C16	21	0.11	83	8.9	8.2	...	...	...	...
C1	21	0.10	83	8.1	0.4	371	60	272	110

Toughnesses denoted (...) are for specimens that had not failed by cleavage fracture up to the amount of crack extension indicated.

Table 5 Summary of results for 1T SE(B) specimens with a/W=0.5 and 0.1.

ID	Temp. (C)	a/W	W (mm)	a_o (mm)	Δa (mm)	J_{crit} (kJ/m^2)	J_{SSY} (kJ/m^2)	K_{Jcrit} (MPa-m$^{1/2}$)	K_{Jssy} (MPa-m$^{1/2}$)
B9B	-7	0.56	51	28	0.6	266	129	230	160
B9C	-7	0.57	51	29	0.1	133	102	163	142
B14C	-7	0.56	51	28	0.3	252	128	224	160
B14B	-7	0.56	51	28	0.8	377	140	274	167
B9A	-7	0.56	51	28	0.4	238	126	218	159
B14A	-7	0.56	51	28	0.3	248	127	223	159
B1A	-7	0.56	51	28	0.3	207	121	204	156
A7B	-7	0.14	51	7.0	0.8	428	54	293	104
B7A	-7	0.13	51	6.7	1.7	653	68	361	117
B11B	-7	0.13	51	6.6	0.2	187	32	193	80
B12B	-7	0.14	51	7.2	0.7	525	61	324	110
B4A	-7	0.14	51	7.3	3.7	1364	80	522	127
B7B	-7	0.14	51	7.0	0.3	241	28	219	87
B11A	-7	0.13	51	6.8	1.2	588	65	343	114

above, and converted to K_{Jc} using:

$$K_{J_c} = \sqrt{EJ_c} \tag{19}$$

where E is the material elastic modulus. A special form of a three-parameter Weibull distribution is fit to the data, i.e.,

$$P_f = 1 - \exp - \left[\frac{(K_{J_c} - K_{min})}{(K_o - K_{min})} \right]^m \tag{20}$$

in which two of the three Weibull parameters have been chosen, that is K_{min} = 20 MPa$\sqrt{m}$ and m = 4, leaving only the scale value K_o. This equation can be fit to data by taking the natural logarithm of both sides twice to give:

Table 6 Summary of results for 1T SE(T) specimens with a/W=0.4.

ID	Temp. (C)	a/W	W (mm)	a_o (mm)	Δa (mm)	J_{crit} (kJ/m^2)	J_{SSY} (kJ/m^2)	K_{Jcrit} (MPa-m$^{1/2}$)	K_{Jssy} (MPa-m$^{1/2}$)
LS-10	-62	0.36	64	22.7	0.1	71	48	119	99
US-13	-62	0.37	64	23.7	0.0	37	30	86	77
LS-3	-7	0.35	64	22.3	0.4	341	129	261	161
LS-7	-7	0.40	64	25.5	2.3	764	205	391	202
LS-11	-7	0.36	64	22.8	1.0	437	149	296	172
US-3	-7	0.36	64	22.7	0.1	192	91	196	135
US-4	-7	0.36	64	23.1	0.5	266	111	231	149
US-5	-7	0.36	64	23.2	0.1	66	46	115	95
US-9	-7	0.35	64	22.0	0.9	550	172	332	186
LS-1	21	0.37	64	23.5	1.0	386	137	278	166
LS-14	21	0.36	64	22.8	1.1	444	150	298	173
US-6	21	0.36	64	23.0	1.1	605	181	348	190
US-10	21	0.36	64	23.2	1.0	443	149	298	173
US-15	21	0.40	64	25.2	0.2	280	111	237	149
US-11	21	0.37	64	23.2	0.5	288	116	240	152
US-7	21	0.38	64	24.3	5.6	816	216	404	208

$$\ln\left[\ln\left(\frac{1}{1-P_f}\right)\right] = 4\ln(K_{J_c} - 20) - 4\ln(K_o - 20) \qquad (21)$$

This is the equation of a straight line having a slope of 4, with the scale value K_o present in the intercept.

3.3 Applications of the Procedure

A typical data set is shown in Figure 6. Data comparisons are best made using a standard thickness specimen, and the recommended test practice uses the 1T or 25 mm thickness specimen. For specimens that are of different thickness an adjustment is made

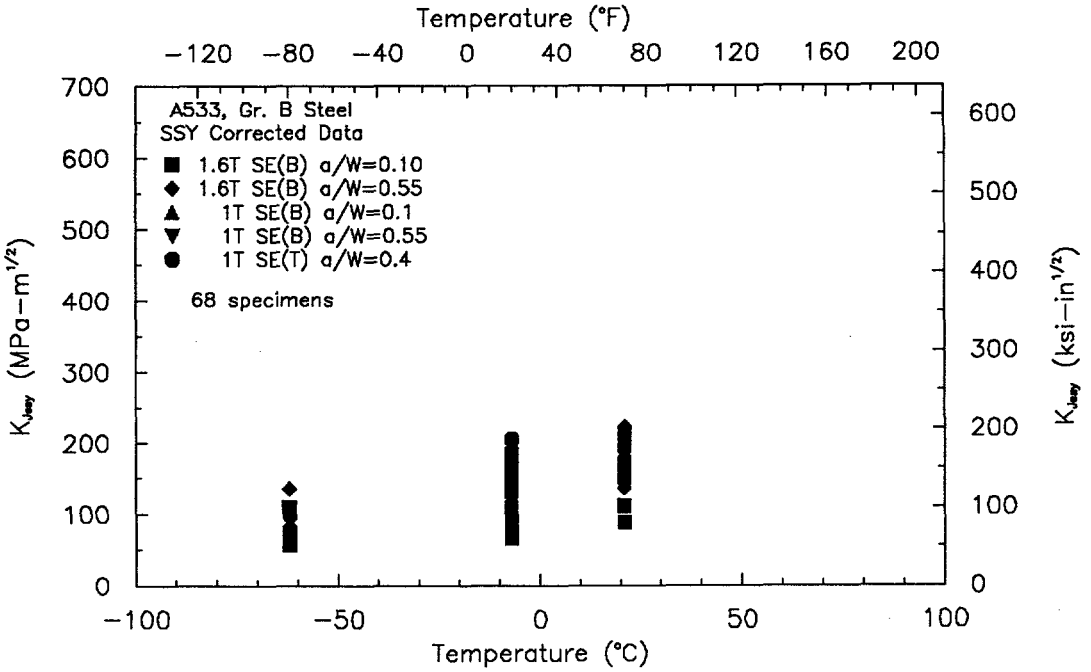

Figure 5 Constraint-corrected fracture toughness values from all tests conducted in this investigation.

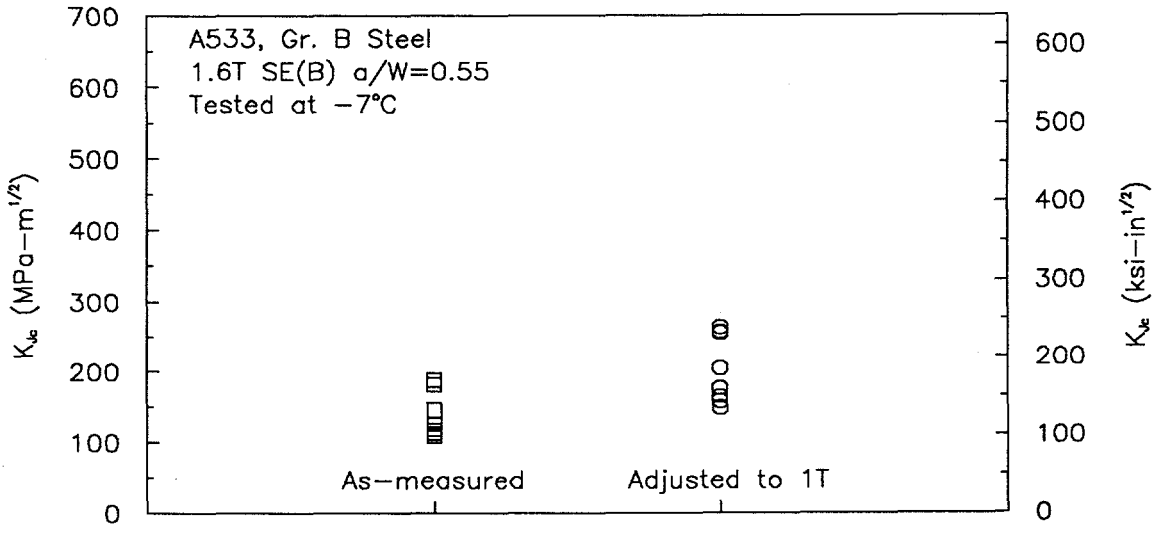

Figure 6 Fracture toughness results for 1.6T SE(B) specimens, a/W=0.55, tested at -7°C.

according to the following equation:

$$K_{Jc(1T)} = 20 + [K_{Jc(x)} - 20]\left(\frac{B_o}{25.4}\right)^{1/4} \tag{22}$$

where B_o is the specimen thickness in mm and the fracture toughness is in MPa$\sqrt{m}$. The results for the 1.6T specimens were adjusted to a 1T thickness using the above expression and the results are also shown in Figure 6.

The required fitting parameter, K_o, can be obtained from the intercept, b, of a least squares linear regression analysis of the data set, which is equivalent to:

$$b = \frac{\sum y_i - 4\sum x_i}{n} \tag{23}$$

where n is the number of data available. For the example shown in Figure 7, with 8 data points:

$$b = \frac{-4.113 \; -4(40.346)}{8} = -20.69 \tag{24}$$

and b = -20.69 = -4ln(K_o - 20), or K_o = 196.2 MPa$\sqrt{m}$.

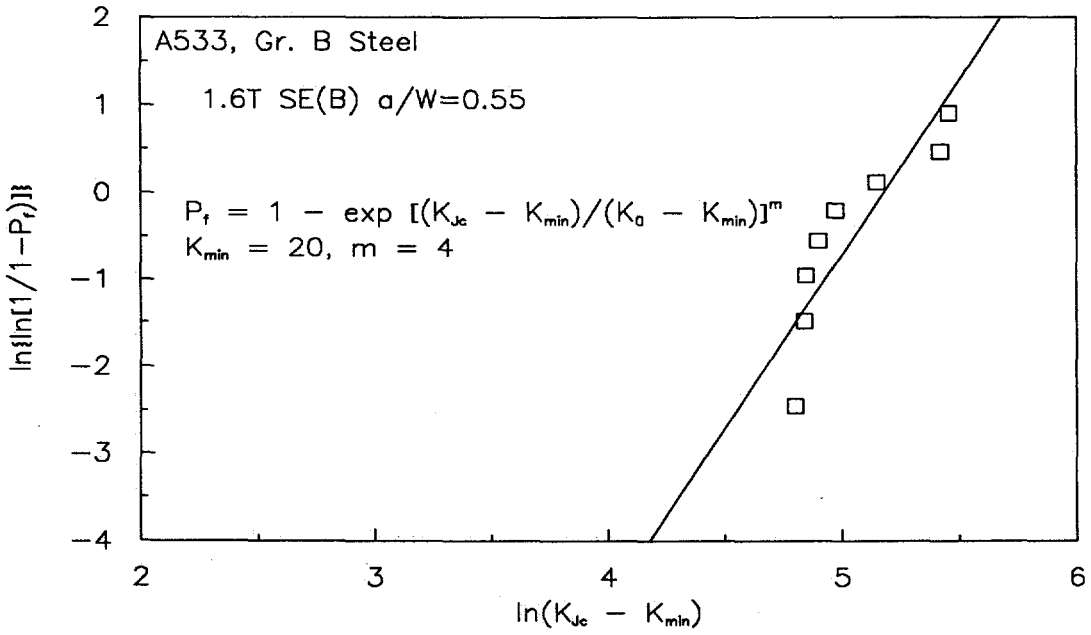

Figure 7 Weibull plot for 1.6T SE(B) specimens tested at -7°C. Data has been constraint-corrected.

The test procedure then evaluates a median $K_{Jc(Med)}$ quantity using Eq. 20 at P_f = 0.5 to give, for the example data set above:

$$K_{Jc(Med)} = [\ln(2)]^{1/4}(K_o - 20) + 20 \quad MPa\sqrt{m} = 180.8 \ MPa\sqrt{m} \tag{25}$$

The draft ASTM test practice defines a master curve, giving $K_{Jc(Med)}$ as a function of temperature throughout the lower and mid-transition, which is assumed to be of the form:

$$K_{Jc(Med)} = 30 + 70 \exp[0.019(T - T_o)] \quad MPa\sqrt{m} \tag{26}$$

where T_o is the temperature at which a 1T size specimen should have a median value of 100 MPa$\sqrt{}$m. For the above case the value of $K_{Jc(Med)}$ found in Eq. 25 can be substituted into Eq. 26 to give T_0 = -47C. The final master curve for this case according to the test practice is thus:

$$K_{Jc(Med)} = 30 + 70 \exp[0.019(T + 47)] \quad MPa\sqrt{m} \tag{27}$$

This equation is shown on Figure 8 plotted with the data set from which it was obtained.

Confidence limits can be calculated, as proposed in the ASTM test practice, by recognizing that for special Weibull distribution of Eq. 20, the standard deviation is given by:

$$\sigma = 0.28 K_{Jc(Med)} - 5.6 \tag{28}$$

and standard normal deviates for the 95% confidence interval can be obtained as:

$$Z_{95} = \frac{[0.478 K_{Jc(Med)} - 10.5]}{\sigma} \tag{29}$$

At a particular temperature, upper and lower K_{95} values can be obtained from:

$$K_{95} = K_{Jc(Med)} \pm Z_{95}\sigma \tag{30}$$

Confidence limits for the example case are shown in Figure 8.

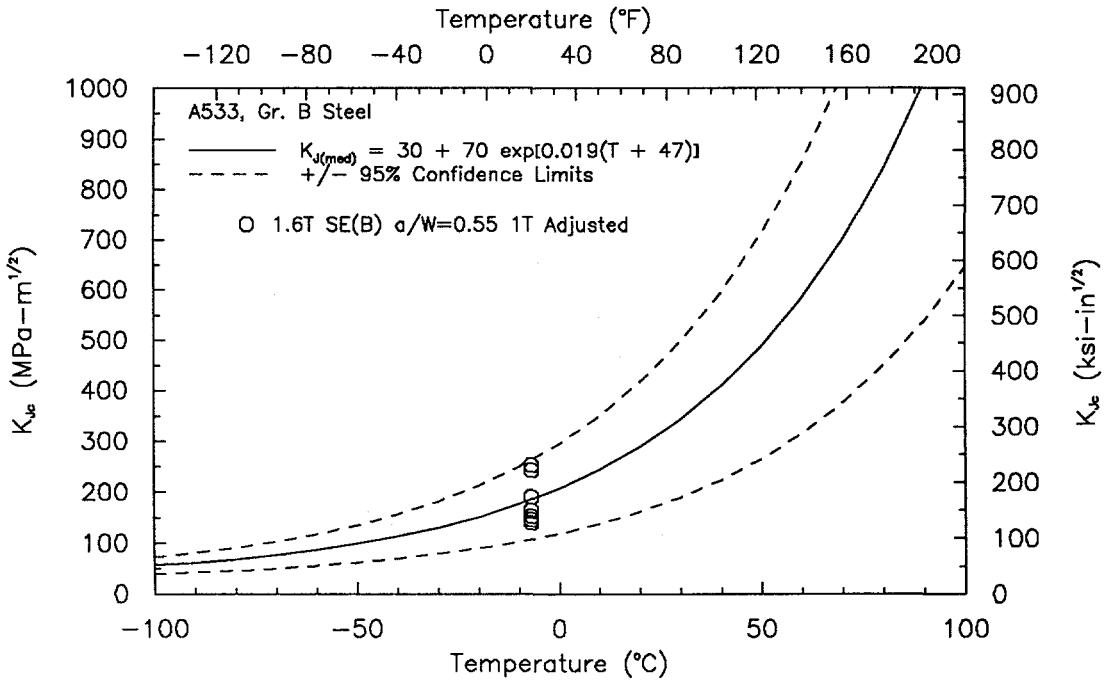

Figure 8 Master curve obtained from 1.6T SE(B) specimens tested at -7°C.

4.0 DISCUSSION

4.1 Discussion of the Experimental Results

In this study the deeply notched 1.6T SE(B) specimens tested at -7°C are used as the baseline data set since, in general, they do not need to be SSY corrected because of their deep notch bend configuration, large size, and low toughness. (Two points did need a correction, amounting to a reduction of approximately 10% on the K_{Jc} values and an increase in T_o of 3°C). All other data sets will be compared, in turn, with this baseline data set. The baseline data set was the data set used in the previous section for the example ASTM test practice calculation, and the baseline result, with the corresponding 95% confidence interval is shown in Figure 8. Figure 9 shows a comparison of the -62°C and 21°C large, deep notched specimens with the baseline median curve and confidence limits. At 21°C some specimens have developed very high K_{Jc} values before cleavage, and the constraint correction procedure must be applied to these values to obtain comparable $K_{J(SSY)}$ results. Corrected results are shown in Figure 10. The results agree well with the master curve only at -7°C, being above the master curve at -62°C and below the master curve at 21°C.

Similarly, Figure 11 shows 1T thickness adjusted and SSY corrected data for the short cracked, 1.6T, SE(B) specimens tested at -62°C, -7°C, and 21°C, along with the baseline master curve and 95% confidence interval. For this case, large constraint corrections are required for most specimens at all temperatures. Note that the constraint corrected data falls below the master curve except at the -62°C temperature.

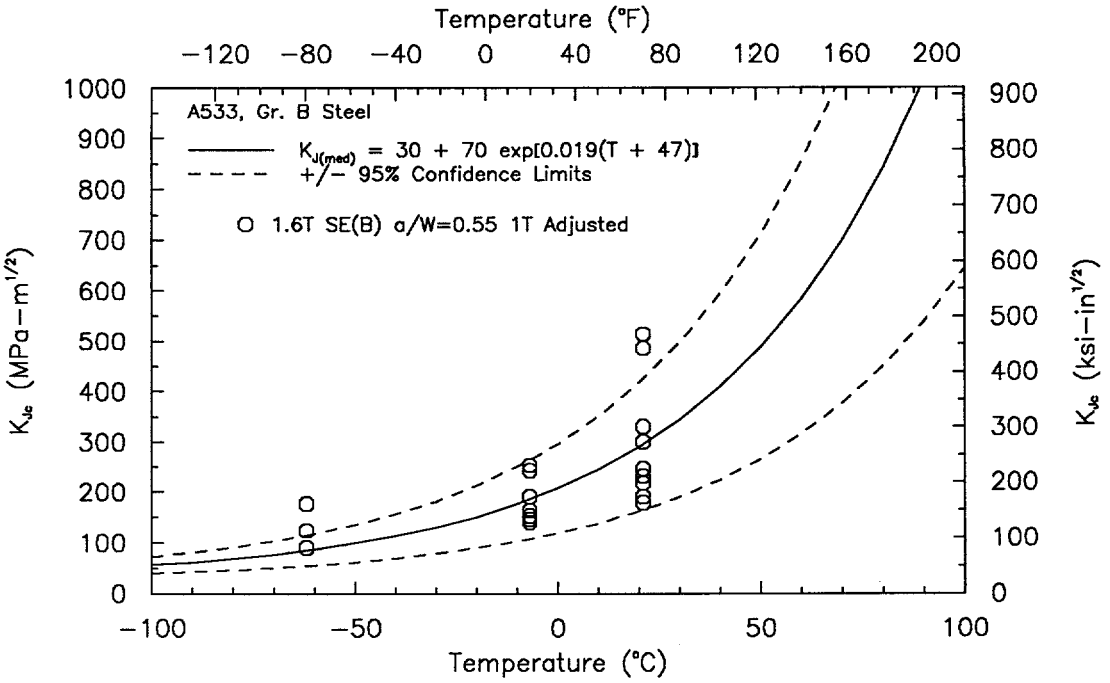

Figure 9 Comparison of the fracture toughness measured at -62°C and 21°C with the master curve and confidence limits for the deeply notched 1.6T SE(B) specimens.

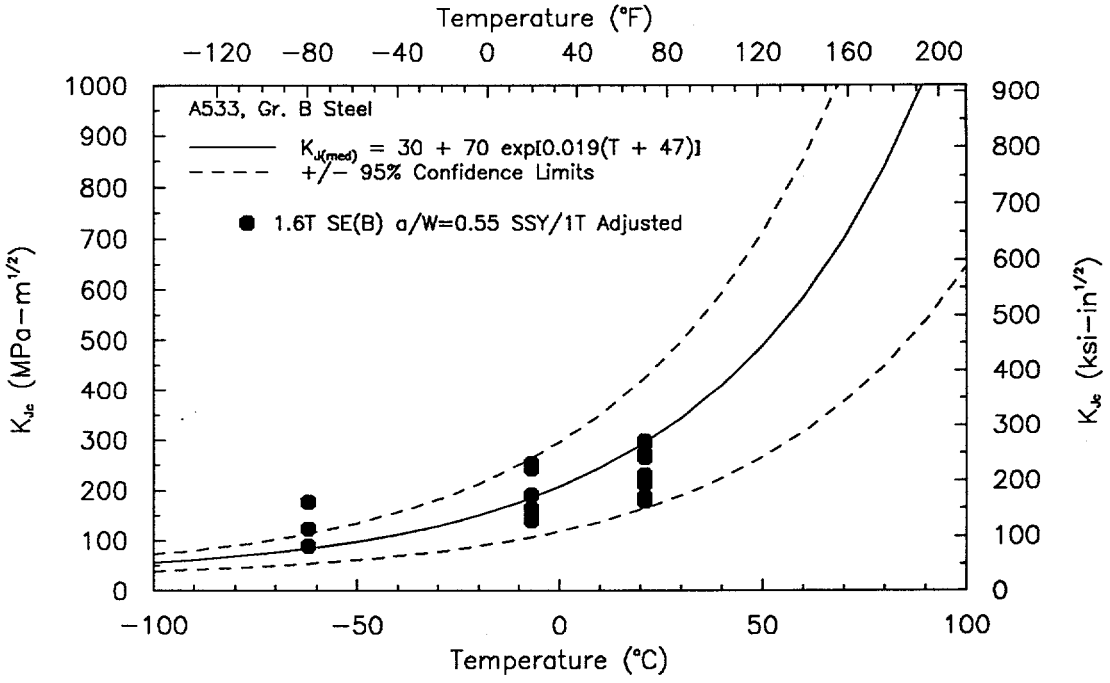

Figure 10 Constraint corrected cleavage fracture toughness results from deeply cracked, 1.6T SE(B) specimens.

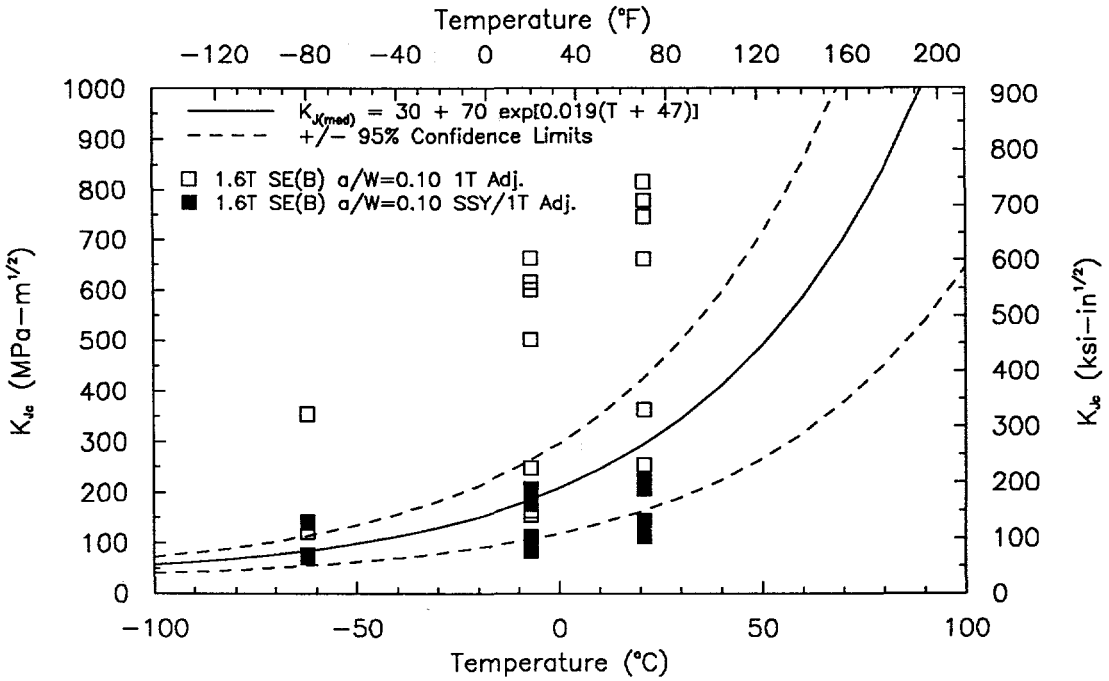

Figure 11 As-measured and constraint-corrected fracture toughness results for shallow cracked 1.6T SE(B) specimens.

Figure 12 and Figure 13 show similar plots for the SE(T) specimens tested at -62°C, -7°C and 21°C and the deep and short notched 1T SE(B) specimens, all of which were tested at -7°C. Both uncorrected and constraint corrected data are plotted in these figures. The highly elevated data is brought into the master curve confidence range, but it seems to invariably lie on the lower side of what is intended to be the median toughness curve. Many of the specimens tested at 21°C have demonstrated significant ductile crack growth (> 0.25 mm) before cleavage initiation, and for these specimens the constraint correction might be too large, which could account for some of the observed tendency for the data to fall below the ASTM master curve. This is not the case for the data at -7°C; however, and this data still falls predominantly below the master curve.

An alternative possibility is that the ASTM master curve, which is not referenced in the present ASTM test practice rough draft, was obtained from specimens which were too small, i.e. data that should have had a constraint correction, but did not, resulting in a master curve that is elevated, and hence non-conservative. A modified master curve was developed in this study from the constraint corrected 1.6T SE(B) data at -7°C and 21°C, as shown in Figure 14, by adjusting the coefficient in the exponential function, and the corresponding T_o until a best fit was obtained at both temperatures, giving a modified master curve of the form:

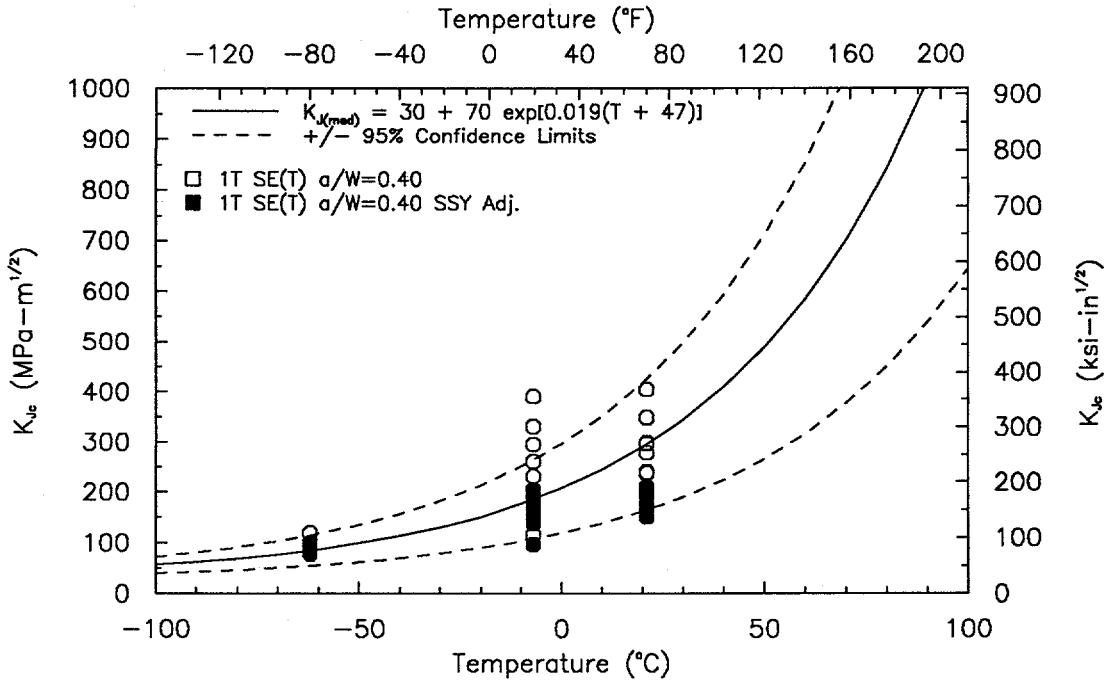

Figure 12 As-measured and constraint-corrected fracture toughness results for 1T SE(T) specimens, a/W=0.4 compared with master curve from 1.6T SE(B) specimens.

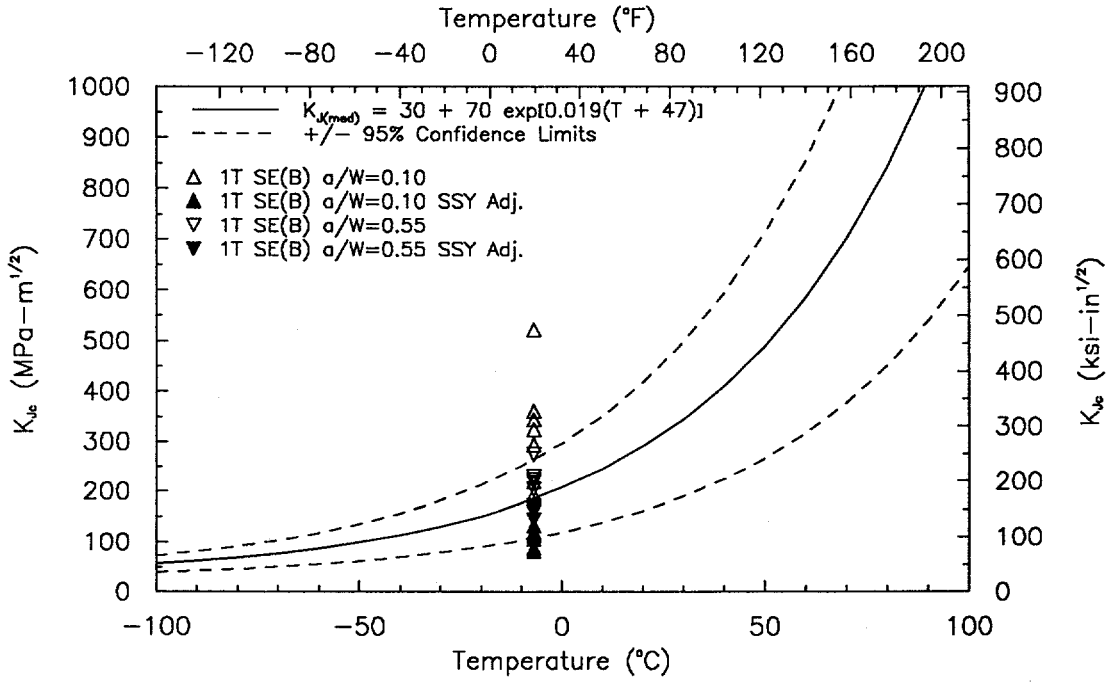

Figure 13 As-measured and constraint corrected fracture toughness results for shallow crack 1T SE(B) specimens compared with master curve from 1.6T SE(B) specimens.

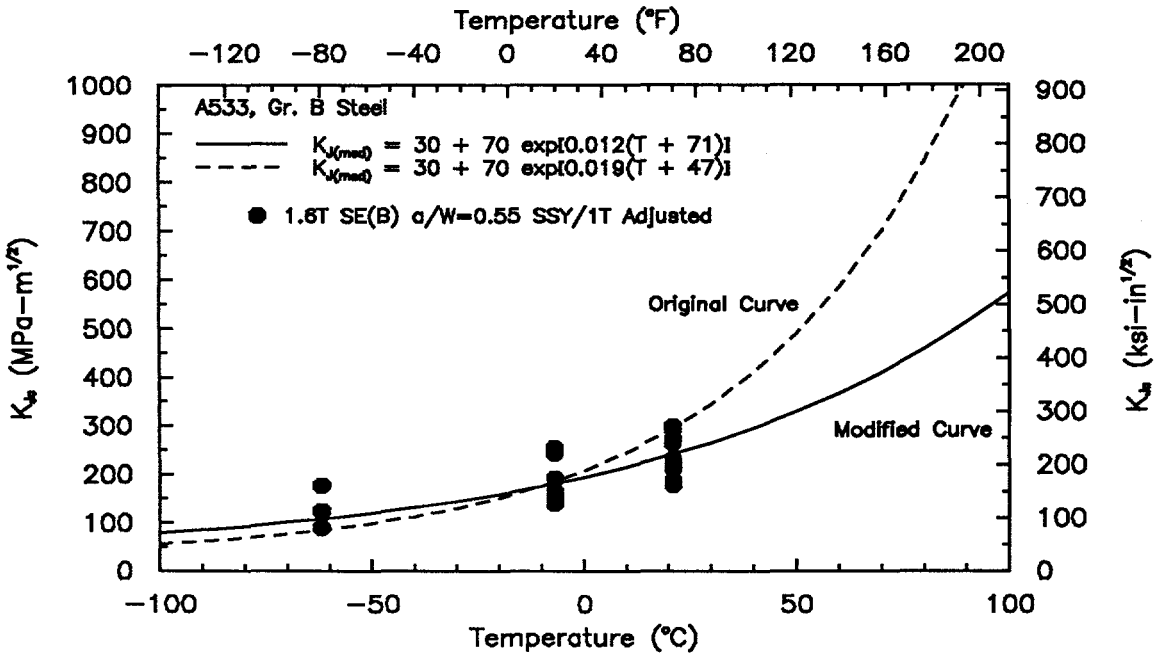

Figure 14 Comparison of original master curve and the modified master curve developed for deeply cracked 1.6T SE(B) specimens.

$$K_{Jc(Med)} = 30 + 70\exp[0.012(T - T_o)] \quad (31)$$

where, for this case, T_o = -71°C. As shown in Figure 15, this modified master curve fits the SSY constraint corrected data much better than the suggested ASTM master curve.

An unresolved issue regarding transition range fracture data concerns the proper way to handle the results from specimens tested in the transition region that do not fail by cleavage initiation. Two of the shallow crack, 1.6T SE(B) specimens tested at 21°C did not fail by cleavage initiation, even after stable ductile crack extension in excess of 8 mm. These results were not considered in any of the previous comparisons, but clearly the toughnesses measured in these specimens are as valid as the results from specimens that did fail by cleavage. At the present time, there does not seem to be any satisfactory way to incorporate this data into a statistical treatment of the data set.

The ASTM proposed test practice does not presently include a constraint correction, and this is viewed as a major shortcoming by the present authors. Without such a correction, the Weibull analysis is being asked to account for variability in the K_J values that is due to crack tip constraint, as well as the statistical variability in the true material toughness that is due to the relative position of the crack tip and the cleavage fracture initiation site.

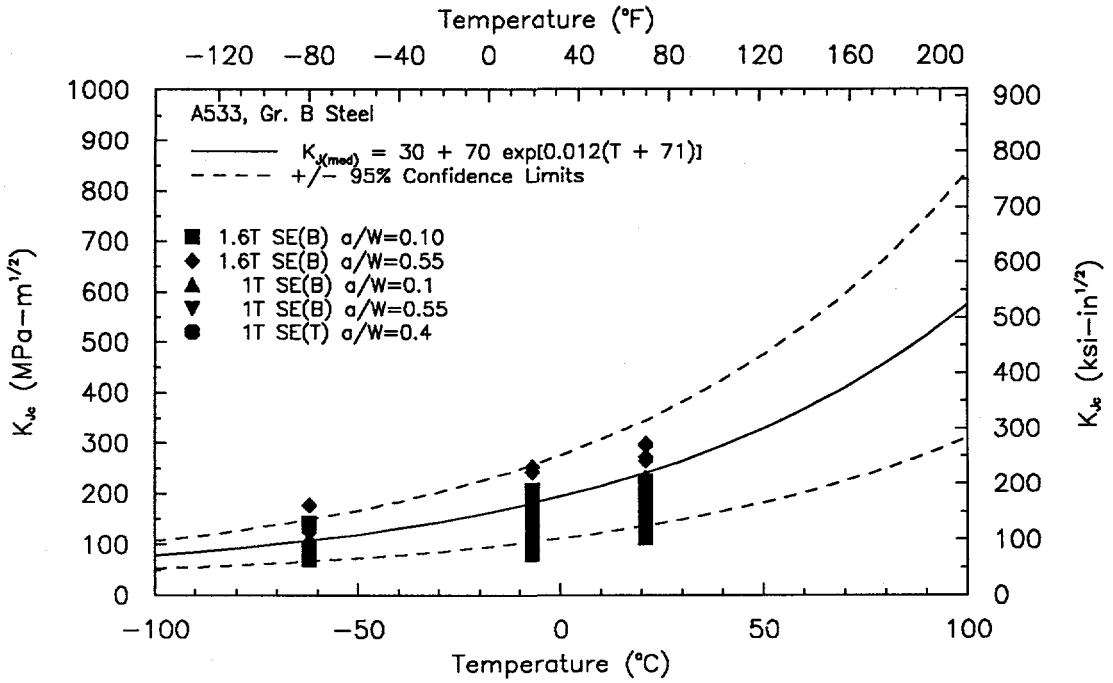

Figure 15 Comparison of all fracture toughness results with the modified master curve and corresponding +/-95% confidence limits.

4.2 Discussion of the Toughness Correction Models

The cleavage toughness scaling models have usually been evaluated by correcting data from subsize and or shallow cracked specimens for comparison with data from deeply cracked bend specimens that do not require a constraint correction. An alternative approach for evaluating the toughness scaling models is to use the scaling models to predict the toughness that a subsize or shallow cracked specimen would exhibit. This approach may more accurately reflect the manner in which the scaling models would be used to predict the performance of a large structure containing a shallow crack.

The following procedure was employed to predict the actual measured fracture toughness in the shallow cracked SE(B) specimens and the SE(T) specimens. The modified master curve and 95% confidence limits developed in the previous section was assumed to accurately describe the transition fracture toughness of the A533B steel. The curves were adjusted to account for a difference in specimen thickness using equation (22) which has been rearranged to give:

$$K_{Jc(x)} = 20 + \left[K_{Jc(1T)} - 20\right]\left(\frac{25.4}{B_x}\right)^{1/4} \qquad (32)$$

where B_x is the specimen thickness in mm and $K_{Jc(x)}$ is the toughness adjusted from a 1T size to the actual thickness of the specimen tested.

The constraint-correction procedure is then employed in reverse using the curves from Figure 3 to calculate the value of toughness, J_{FB}, that would be expected in a specimen with a different crack size or geometry. By "uncorrecting" the median and 95% confidence limit curves in this manner, it is possible to predict the actual toughness measured in the short crack SE(B) and the SE(T) specimens.

An example of the prediction for the 1T SE(T) specimens is shown in Figure 16. In this case, the actual specimen was a 1T specimen, so equation (32) was not applied. The modified master curve, adjusted for loss of constraint by the scaling models, provides a reasonable prediction of the measured toughnesses, with all but one data point falling within the 95% confidence limits; however, most of the data fall below the predicted median curve. Another example is shown in Figure 17 where the 1.6T SE(B), a/W=0.1 results are predicted. The scaling models predict the correct trends in the data -- increased scatter and toughness, but there are many points at or below the -95% confidence limit. This indicates that the scaling model is predicting a greater increase in toughness due to a loss of constraint than is actually observed for this material. This is an important point with regard to assessing toughness scaling models. A scaling model that over-corrects measured toughness in a low constraint specimen relative to a high constraint specimen will also over-predict the increase in toughness that a low constraint structure may exhibit.

There are several possible reasons why the constraint corrections are over-correcting the data from the short cracked specimens. These include three-dimensional

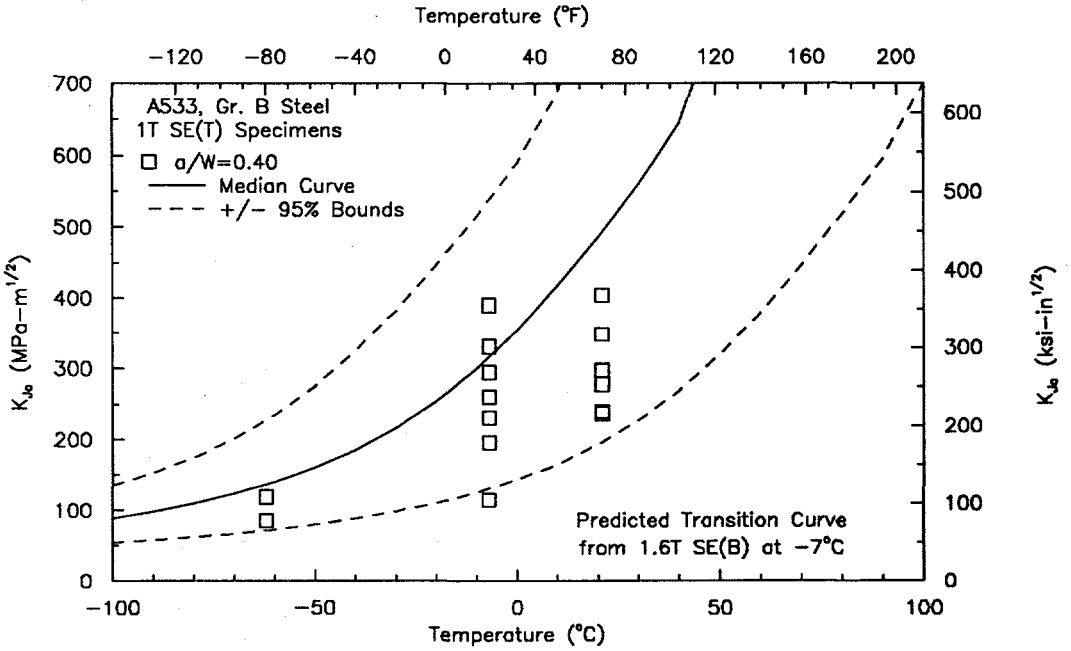

Figure 16 Comparison of the predicted median and 95% confidence limits with the measured cleavage fracture toughness for 1T SE(T) specimens with a/W=0.4.

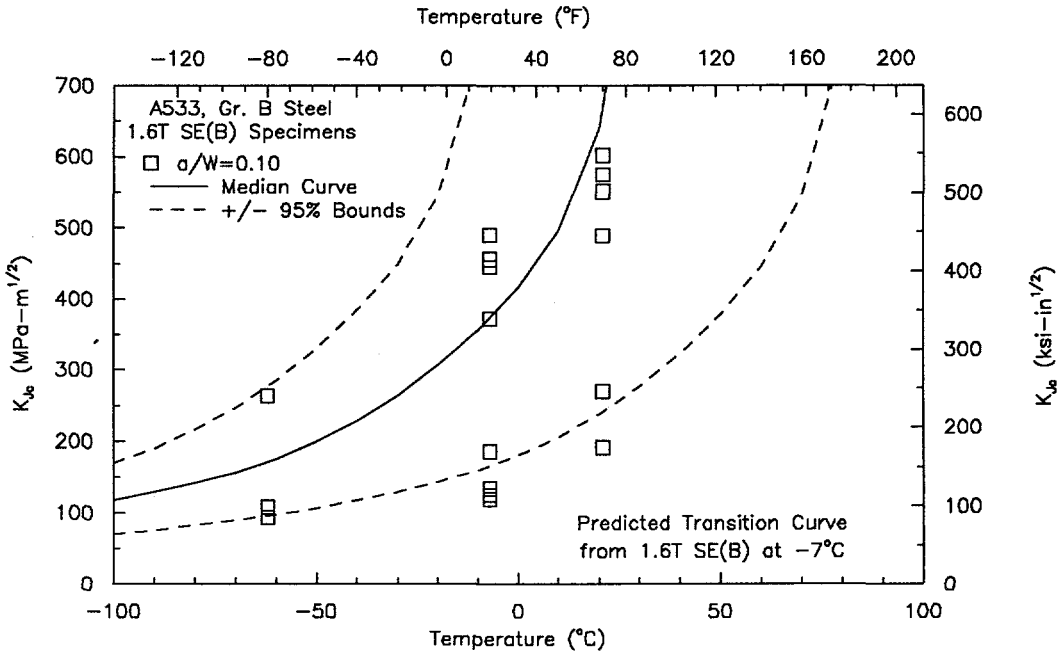

Figure 17 Comparison of the predicted median and confidence limits with the measured cleavage fracture toughness for 1.6T SE(B) specimens with a/W=0.1.

effects which were not incorporated into the models employed in this study, the effects of ductile tearing prior to cleavage crack initiation or some mechanism other than a strictly stress-controlled mechanism that dictates when cleavage cracking will initiate. The specimens used in this investigation had side-grooves to help control the crack front straightness during ductile crack extension. The sidegrooves have been shown [12] to promote plane strain behavior, but the effects of the sidegrooves has not been explicitly incorporated into the development of the scaling models. Observations of the fracture surfaces of the short crack specimens did not indicate that the cleavage initiation sites were influenced by the side-grooves.

Other investigators have shown that constraint corrections tend to over correct data from subsize specimens that have significant ductile tearing prior to cleavage initiation [13]. Techniques are only now being developed that incorporate the effects of stable ductile tearing on constraint correction procedures [13]. In any case, all of the short cracked SE(B) specimens which had little or no crack growth prior to cleavage initiation fall below the deep crack SE(B) results after the constraint correction has been applied. Therefore an additional correction to account for crack growth would not improve the situation.

The results of this investigation show that the cleavage fracture toughness scaling models over-predict the elevation in fracture toughness that results from shallow cracks in large specimens. It is reasonable to expect that these scaling models would lead to

non-conservative assessments of RPV integrity if they are used to take advantage of the so-called "short crack" effect.

5.0 CONCLUSIONS

A large number of specimens varying in both specimen size and geometry were tested at several temperatures in the ductile-brittle transition region for a heat treated A533, Grade B steel plate. Constraint corrections, based on a cleavage fracture toughness scaling model were applied to the results and the constraint corrections were effective in reducing the scatter in the results by a significant margin. The proposed ASTM test practice statistics-based procedure was used to analyze the results. This procedure relies on the use of a master curve and the associated confidence limits for describing the transition behavior of materials. All results were constraint-corrected in this study and it was found that the ASTM proposed master curve was non-conservative in predicting mid-transition and upper transition behavior when fit to low transition data. An improved expression for the master curve was developed to describe the median fracture toughness as a function of temperature. The modified master curve more accurately models the median toughness at the upper and lower end of the transition region than the original master curve for this material.

The cleavage fracture toughness scaling models tended to over correct the data from shallow cracked specimens when the data were corrected to equivalent J_{ssy} or $K_{J(ssy)}$ values. For the same reason, the scaling models tended to over predict the increase in toughness that a shallow cracked specimen would exhibit. The scaling models should be investigated more thoroughly to determine the basis for this behavior since it can lead to non-conservative predictions when using data from deep crack specimens to predict the performance of RPV structures containing shallow cracks. The toughness scaling models used in this study were developed from 2-D plane strain finite element models of the fracture toughness specimens. The 2-D plane strain models cannot fully capture the inherently 3-D nature of the crack tip fields in finite specimen geometries. Cleavage fracture toughness scaling models based on 3-D analyses which are currently under development may show less tendency to over-correct the fracture toughness of the shallow cracked specimens.

REFERENCES

[1] Anderson, T.L. and Dodds, R.H., Jr., "Specimen Size Requirements for Fracture Toughness Testing in the Transition Region," *Journal of Testing and Evaluation*, JTEVA, Vol. 19, No. 2, March 1991, pp. 123-134.

[2] Dodds, R.H., Jr., Anderson, T.L., and Kirk, M.T., "A Framework to Correlate a/W Ratio Effects on Elastic-plastic Fracture Toughness (J_c)," *International Journal of Fracture*, Vol. 48, 1991, pp. 1-22.

[3] Shih, C.F., O'Dowd, N.P. and Kirk, M.T., "A Framework for Quantifying Crack Tip Constraint," *Constraint Effects in Fracture, ASTM STP 1171*, E.M. Hackett, K.H. Schwalbe and R.H. Dodds, Eds., American Society for Testing and Materials, Philadelphia, 1993, pp. 2-20.

[4] Kirk, M. T., Koppenhoefer, K. C., and Shih, C. F., "Effect of Constraint on Specimen Dimensions Needed to Obtain Structurally Relevant Toughness Measures." *Constraint Effects in Fracture, ASTM STP 1171*, E. M. Hackett, et al., Eds., American Society for Testing and Materials, Philadelphia, 1993, pp. 79-103.

[5] Sumpter, J. D. G. and Forbes, A.T., "Constraint Based Analysis of Shallow Cracks in Mild Steel", Proceedings of TWI/EWI International Conference on Shallow Crack Fracture Mechanics, Toughness Tests and Applications, Cambridge, UK, 1992.

[6] Anderson, T.L., Vanaparthy, N.M.R. and Dodds, R.H., Jr., "Predictions of Specimen Size Dependence on Fracture Toughness for Cleavage and Ductile Tearing," *Constraint Effects in Fracture, ASTM STP 1171*, E. M. Hackett, et al., Eds., American Society for Testing and Materials, Philadelphia, 1993, pp. 473-491.

[7] Joyce, J.A., "J-Resistance Curve Testing of Short Crack Bend Specimens Using Unloading Compliance," *Fracture Mechanics: Twenty-Second Symposium (Volume I), ASTM STP 1131*, H.A. Ernst, A. Saxena, and D.L. McDowell, Eds., American Society for Testing and Materials, Philadelphia, 1992, pp. 904-924.

[8] Joyce, J.A., Hackett, E.M. and Roe, C., "Effects of Crack Depth and Mode of Loading on the J-R Curve Behavior of a High-Strength Steel", *Constraint Effects in Fracture, ASTM STP 1171*, E. M. Hackett, et al., Eds., American Society for Testing and Materials, Philadelphia, 1993, pp. 239-263.

[9] Hackett, E.M and Joyce, J.A., "Dynamic J-R Curve Testing of a High Strength Steel Using the Key Curve and Multi-Specimen Techniques," *Fracture Mechanics, ASTM STP 905*, American Society for Testing and Materials, Philadelphia, 1986, pp. 741-774.

[10] Haigh, J.R. and Richards, C.E., "Yield Point Loads and Compliance Functions of Fracture Mechanics Specimens," CEGB Report RD/L/M461, Central Electricity Generating Board, UK, 1974.

[11] Sumpter, J.D.G., "J_c Determination for Shallow Notch Welded Bend Specimens," *Fatigue and Fracture of Engineering Materials and Structures*, Vol. 10, No. 6, 1987, pp. 479-493.

[12] DeLorenzi, H.G. and Shih, C.F., "3-D Elastic-Plastic Investigation of Fracture Parameters in Side-Grooved Compact Specimens," *International Journal of Fracture*, Vol. 21, pp. 1983, 195-220.

[13] Dodds, R.H., Jr. and Anderson, T.L., "Effects of Ductile Tearing on Crack-Tip Constraint in Single-Edge Notched Bend Specimens," *Constraint Effects in Fracture: Theory and Applications, ASTM STP 1244*, Mark Kirk and Ad Bakker Eds., American Society for Testing and Materials, Philadelphia, 1994.

NRC FORM 335 (2-89) NRCM 1102, 3201, 3202

U.S. NUCLEAR REGULATORY COMMISSION

BIBLIOGRAPHIC DATA SHEET

(See instructions on the reverse)

1. REPORT NUMBER (Assigned by NRC, Add Vol., Supp., Rev., and Addendum Numbers, if any.)
NUREG/CR-6279

2. TITLE AND SUBTITLE
Application of Fracture Toughness Scaling Models to the Ductile-to-Brittle Transition

3. DATE REPORT PUBLISHED
MONTH: Janaury
YEAR: 1996

4. FIN OR GRANT NUMBER
J6036

5. AUTHOR(S)
R. E. Link, Naval Surface Warfare Center
J. A. Joyce, U.S. Naval Academy

6. TYPE OF REPORT
Technical

7. PERIOD COVERED *(Inclusive Dates)*
Sept 1992 - Sept 1994

8. PERFORMING ORGANIZATION – NAME AND ADDRESS *(If NRC, provide Division, Office or Region, U.S. Nuclear Regulatory Commission, and mailing address; if contractor, provide name and mailing address.)*

Naval Surface Warfare Center
3-A Leggett Circle
Annapolis, MD 21402

U.S. Naval Academy
590 Holloway Road
Annapolis, MD 21402

9. SPONSORING ORGANIZATION – NAME AND ADDRESS *(If NRC, type "Same as above"; if contractor, provide NRC Division, Office or Region, U.S. Nuclear Regulatory Commission, and mailing address.)*
Division of Engineering Technology
Office of Nuclear Regulatory Research
U.S. Nuclear Regulatory Commission
Washington, DC 20555-0001

10. SUPPLEMENTARY NOTES
S. N. Malik, NRC Project Manager

11. ABSTRACT *(200 words or less)*

An experimental investigation of fracture toughness in the ductile-brittle transition range was conducted. A large number of ASTM A533, Grade B steel, bend and tension specimens with varying crack lengths were tested throughout the transition region. Cleavage fracture toughness scaling models were utilized to correct the data for the loss of constraint in short crack specimens and tension geometries. The toughness scaling models were effective in reducing the scatter in the data, but tended to over-correct the results for the short crack bend specimens. A proposed ASTM Test Practice for Fracture Toughness in the Transition Range, which employs a master curve concept, was applied to the results. The proposed master curve over predicted the fracture toughness in the mid-transition and a modified master curve was developed that more accurately modeled the transition behavior of the material. Finally, the modified master curve and the fracture toughness scaling models were combined to predict the as-measured fracture toughness of the short crack bend and the tension specimens. It was shown that when the scaling models over correct the data for loss of constraint, they can also lead to non-conservative estimates of the increase in toughness for low constraint geometries.

12. KEY WORDS/DESCRIPTORS *(List words or phrases that will assist researchers in locating the report.)*
Cleavage, Transition, Fracture, Toughness, Statistical Models, Ductile Tearing, Brittle Fracture, Fracture Testing

13. AVAILABILITY STATEMENT
Unlimited

14. SECURITY CLASSIFICATION
(This Page)
Unclassified
(This Report)
Unclassified

15. NUMBER OF PAGES

16. PRICE